Mutation in *TMEM98* in a Large White Kindred with Autosomal Dominant Nanophthalmos Linked to 17p12-q12

Mona S Awadalla, MMBS, PhD[1] *

Kathryn P Burdon, PhD[1]*

Emmanuelle Souzeau, MSc[1]

John Landers, MBBS, MPH, PhD[1]

Alex W. HewittMBBS, PhD [2]

Shiwani Sharma, PhD[1]

Jamie E Craig, MBBS, DPhil[1]

[1] Department of Ophthalmology, Flinders University, Flinders Medical Centre Adelaide, South Australia, Australia.

[2] Centre for Eye Research Australia, Royal Victorian Eye and Ear Hospital, University of Melbourne, Melbourne, Victoria, Australia

* Contributed equally

Corresponding Authors

Kathryn P Burdon, PhD

Menzies Research Institute Tasmania, University of Tasmania, Private Bag 23, Hobart, TAS, 7001, Ph 03 62264288, Email Kathryn.burdon@utas.edu.au

Jamie E Craig

Ophthalmology Department, Flinders University, GPO Box 2100, Adelaide South Australia, Australia 5000. Fax: +61 8 8277 0899; email: jamie.craig@flinders.edu.au

Word count: 3,000

Abstract

Importance:

Nanophthalmos is a congenital disorder characterised by small eyes, with the main complications being severe hyperopia and angle-closure glaucoma.

Objective: To perform a clinical and genetic investigation of a large White family with autosomal dominant nanophthalmos.

Design, setting, and Participants:

Detailed clinical evaluation and a genome-wide linkage scan was conducted in the family, NNO-SA1. Linkage was evaluated with a 10K single nucleotide polymorphism array, followed by whole exome sequencing to identify novel segregating coding variants within the linked region. The candidate gene was screened for mutations in additional independent families by direct sequencing of the coding exons and intron/exon boundaries. The expression pattern of the candidate gene in ocular tissues was analysed by reverse transcriptase-polymerase chain reaction.Participants were recruited through Ophthalmology clinics at the Flinders Medical Centre, Adelaide, Australia. Nanophthalmos was defined as an axial length <20.0 mm and/or refractive error >+7.00. Of the 35 available individuals from family NNO-SA1, 16 participants (46%) had a diagnosis of nanophthalmos, with mean refraction of +11 D and mean axial length of 17.5 mm. Unaffected unrelated individuals serving as controls were screened for the identified mutation. Additional independent families with clinically diagnosed nanophthalmos were also recruited.

Main Outcomes and Measures:

Nanophthalmos status

Results:

Significant linkage was detected on chromosome 17 between single nucleotide polymorphism

markers rs2323659 and rs967293 with a maximum location score of 4.1. Exome sequencing identified a single novel segregating missense variant within the linkage region, located in exon 8 of the transmembrane-98 (*TMEM98*) gene c.577G>C (p.Ala193Pro), which was absent in the Exome Variant Server database and among 285 local white individuals serving as controls. The *TMEM98* gene was expressed in all ocular tissues tested including sclera and optic nerve head.

Conclusion and Relevance:

A novel gene associated with nanophthalmos, *TMEM98* most likely represents the cause of the disease in this family. To our knowledge, this represents the first gene identified causing autosomal dominant nanophthalmos.

Introduction

Microphthalmia is a developmental disorder consisting of bilaterally small eyes. Posterior microphthalmia and nanophthalmos are 2 subtypes of the disorder. [1] Nanophthalmos is characterised by the axial length of the globe being more than 2 SDs smaller than the normal range (< 20 mm in adults), [2] and the cornea and lens are typically of normal size, [3] causing severe hyperopia (farsightedness) of +7.00 diopters (D) or more. The smaller dimensions of the anterior chamber depth cause the iridocorneal angle to be typically narrow. Abnormal thickening of the scleral connective tissue is often also observed. [3, 4] The abnormal structure of the anterior chamber observed in nanophthalmos differs from that of posterior microphthalmia, a rare phenotype restricted to the posterior segment of the eye, where the anterior chamber is of normal dimensions. [5-7] A recent study [8] has revealed that eyes with posterior microphthalmia have corneal steepening proportional to the degree of the short axial length, suggesting that both nanophthalmos and posterior microphthalmia are not a distinct phonotype but they represent a spectrum of high hyperopia. The prevalence of all microphthalmia in Australia is between 0.5 and 1.5 per 10,000 births. [9]

Nanophthalmos can be inherited in either an autosomal dominant or autosomal recessive mode. [2, 10] Linkage studies in large families with autosomal dominant nanophthalmos have identified linkage to chromosome 11p in a family from the United States, [11] 2q11-q14 in a Chinese family, [12] and 17p12-q12 also in a Chinese pedigree. [13] To date additional families showing linkage to these regions have not been reported and the causative genes in families with autosomal dominant nanophthalmos have not been identified.

We describe a large family of British ancestry with autosomal dominant nanophthalmos. We conducted genome-wide linkage analysis in this family, localising the gene to a region of

16.9 Mb on chromosome 17 (overlapping with the linkage region in the Chinese family [13]) and investigated the genes in the linked region for causative mutations.

Methods

Recruitment of Participants

Family NNO-SA1 (Figure 1) was identified following presentation of the proband (V:3) to Flinders Medical Centre, Adelaide, Australia for evaluation and treatment related to angle-closure glaucoma. The primary diagnosis of isolated nanophthalmos was made in that setting by one of the authors (J.E.C). The family history of this patient was obtained and the extended family was traced for 5 generations. Thirty-five family members were recruited into the study, 16 of whom received a diagnosis of nanophthalmos. An additional 7 family members were reported to have the same phenotype, but were not available for study. The proband and her immediate family reside in Australia, however much of the extended family is living in the United Kingdom. Written informed consent was obtained from all participants in accordance with the Declaration of Helsinki, and the study was approved by the Southern Adelaide Clinical Human Research Ethics Committee, South Australia.

The proband (V:3) received a full ophthalmic examination including refraction, intraocular pressure, central corneal thickness measurement, slit lamp biomicroscopy, A-scan ultrasonography and optic disc tomography. Angle-closure glaucoma status was assessed in all participants; however, it was not a part of the criteria used to determine affection status. The rest of the family members were classified as having nanophthalmos if they had an axial length less than 20.00 mm and/or a refractive error greater than+7.00. Genomic DNA was extracted from either peripheral whole blood (QiaAmp DNA Blood Maxi Kit; Qiagen) or from saliva (Oragene® DNA Saliva collection kits; DNA Genotek) according to the manufacturers' protocols.

Linkage analysis

All available family members were genotyped (GeneChip Xba 10K single nucleotide polymorphism [SNP] arrays; Affymetrix Inc) at the Australian Genome Research Facility, Melbourne, Australia. Data were provided in the form of linkage format files and analyses were conducted in MERLIN. [14] Because of computational limitations on the number of members of a pedigree, initial genome-wide linkage analysis was conducted using individuals from the proband's branch of the family (descendants of II:1 and II:2), excluding IV:1, V:1, V:2, and V:7, under a fully penetrant dominant model. The disease allele frequency was set to 0.0001 and the allele frequencies for each marker typed were obtained from the CEU (Utah residents with Northern and Western European ancestry from the CEPH (Centre d'Etude Polymorphism Humain) collection) sample of the International HapMap project (http://hapmap.ncbi.nlm.nih.gov/). To confirm the findings, different individuals were excluded and analysis was repeated in the remaining branch of the family (descendants of II:6 and II:7). When the results were compared, only a single region on chromosome 17 showed linkage in both branches. The SNPs surrounding the linked region on chromosome 17 were extracted from the dataset and files were formatted with Mega2 [15] for linkage analysis on the entire pedigree in SimWalk2. [16] A fully penetrant dominant model was used to calculate location scores (equivalent to multi-point logarithm of odds scores) and location scores versus chromosome location were plotted. Haplotypes were reconstructed in MERLIN [14] on sub-sections of the pedigree, with overlapping individuals included in each run to facilitate combining the data into the whole pedigree.

Exome sequencing

Sequencing was performed in 5 individuals selected to represent both main branches of the family: 4 affected individuals (IV:2, IV:5, IV:9, and V:9) and 1 unaffected member (IV:4). Enrichment for the exome was performed (TruSeq Exome Enrichment Kit; Illumina Inc.) and

enriched DNA was sequenced (HiSeq 2000; Illumina Inc) by the Australian Genome Research Facility. Sequence alignment to hg19 was conducted (CASAVA, v1.8.1 (https://support.illumina.com/downloads/casava_181.ilmn), and aligner module ELAND, version 2; Illumina). Realignment and variant calls were made with Illumina Exome Script and variants were annotated by ANNOVAR. [17] All bioinformatics was conducted by the sequencing service provider. The lists of single nucleotide variants identified in each sample were filtered according to the following criteria: (1) not present in dbSNP131, (2) segregated in the 5 sequenced individuals, and (3) missense, stop or splice variant.

Segregation in the family was assessed by Sanger sequencing using primer pair exon 8-1 (eTable 1). Polymerase chain reaction (PCR) was performed for each available DNA sample with the following conditions: enzyme activation at 95ºC for 15 minutes, 30 cycles of denaturation at 95ºC for 30 seconds, annealing at 57ºC for 30 seconds, elongation at 72ºC for 30 seconds, and final elongation at 72ºC for 5 minutes. The PCR products were purified for sequencing using exonuclease l (20U/µL) and USB Shrimp Alkaline Phosphatase (In Vitro Technologies.) (1U/µL), incubate at 37ºC for 60 minutes, and then inactivated at 80ºC for 20 minutes. [18] The product was sequenced using BigDye Terminator; Applied Biosystems on an ABI 3100 DNA sequencer (Applied Biosystems). Chromatograms were compared with each other and the reference sequence (GenBank accession number NM_001033504.1) (Sequencher Software version 5.2.3; http://www.genecodes.com/; GeneCodes Corp).

The presence of the novel missense variant was tested in 285 individuals serving as controls using a restriction fragment length polymorphism. The cohort was ascertained from residential care facilities for the aged in Adelaide, South Australia. The mutation introduces a restriction site for Bsu36I (New England BioLabs Inc.). Polymerase chain reaction was performed with the same primers used for sequencing above. A total of 10 µL of PCR

product was digested with 2U of Bsu36I enzyme in the presence of Bovine Serum Albumin. The digested products were visualized under UV light following electrophoresis on stained agarose gel, 1.4% (Gel Red; biotium). The novel variant was searched against the Exome Variant Server database (http://evs.gs.washington.edu/EVS/), a large public dataset of unrelated European-American individuals with exome sequence data available

The functional significance of the mutation in transmembrane-98 (*TMEM98*; GeneBank NM_001033504.1) was analysed using PolyPhen-2, [19] SIFT using protein ID (ENSP00000261713), [20] and MutationTaster. [21]
The conservation of normal TMEM98 protein was compared between species using data obtained from UniProtKB (http://www.uniprot.org/uniprot/) and aligned by ClustalW2. [22]

Gene screening in additional families with nanophthalmos

A total of 7 additional independent families with at least 1 affected member participated in the present study. Families were referred to the study from eye clinics in Australia. Extraction and sequencing of the DNA of probands were conducted using the same methods as described above with primers for each coding region of the gene, encompassing splice sites (Supplement [eTable 1]).

Expression analysis

Ocular tissues were obtained from post-mortem human eyes through the Eye Bank of South Australia according to the guidelines of the Southern Adelaide Clinical Human Research Ethics Committee. Total RNA was extracted from tissues using the RNeasy Micro Kit or Mini Kit (Qiagen). Primers were designed through National Center for Biotechnology Iinformation/Primer-Blast (http://www.ncbi.nlm.nih.gov/tools/primer-blast/index.cgi?) for

each of the 2 known isoforms: isoform 1 (GeneBank NM_015544) forward primer (5'-3') GCACCTGCCATCCTCTTCCCCA and reverse primer (5'-3') GCAGTCGTCCGTGCGTCCAG, and isoform 2 (GeneBank NM_001033504) forward primer (5'-3') GGGAGCCACAGCCTGAGCTTT and reverse primer (5'-3') AGGAGCAGGGCAGTCGTCCG. First-strand complementary DNA was synthesized using the SuperScript III reverse transcriptase (Invitrogen). Polymerase chain reation was conducted with the following conditions: initialization at 95°C for 15 minutes, followed by denaturation at 95°c for 30 seconds, annealing at 62°C for 30 seconds, elongation at 72°C for 30 seconds for 30 cycles using complementary DNA from retina, optic nerve, optic nerve head, ciliary body, and iris, and 32 cycles for sclera, and then a final elongation at 72°C for 5 minutes. The PCR product was visualised on stained agarose gel, 1.4% (Gel Red; Biotium). Products were purified for sequencing as described above. The publicly available Illumina Human Body-Map, version 2.0, data were accessed on November 19, 2013, through the Ensembl Genome Browse (http://www.ensembl.org) to explore non ocular expression patterns.

Results

Recruitment of Participants

Family NNO-SA1 (Figure 1) presented with autosomal dominant nanophthalmos. Sixteen family members were classified as affected (Table 1). The mean (SD) refraction and axial length of the affected family members were +11.8 (2.5) D and 17.6 (0.6) mm, respectively. Best-corrected visual acuity in these patients ranged from no perception of light to 6/6. Angle-closure glaucoma was detected in 6 of the 16 patients, including the proband (V:3). Individual IV:2 demonstrated slightly elevated pressure but no sign of glaucoma at the time of recruitment. Other clinical features in affected family members included thick sclera with prominent scleral vessels, and an increased frequency of optic disc drusen with some degree

of increased vascular tortuosity. There was also a tendency for aqueous misdirection to occur after intraocular surgery, as well as other complications (eg, macular edema and choroidal effusions), often leading to poor outcomes following intraocular surgery for cataract and glaucoma. Representative images of the ocular phenotype are shown in Figure 2.

Linkage analysis

Linkage analysis in the branch of the pedigree descended from II:1 and II:2 is shown in Figure 3A. Linkage to previously reported nanophthalmos regions on chromosomes 11p [11] and 2q [12] was excluded. Linkage was detected on chromosome 17p12-q12 between SNP markers rs2323659 and rs967293 with a maximum logarithm of odds score of 2.67, overlapping with the region previously identified in the Chinese pedigree. [13] The region was defined by recombination events in individuals III:3 (untyped) and IV:6 (Figure 1). The remaining branch of the family similarly showed linkage to this region on chromosome 17, however no recombinants were observed that would further refine the linkage region. The linked region is approximately 16.9 megabases (Mb) in physical distance between 15.3Mb and 32.7Mb, encompassing the centromere of chromosome 17. Multipoint linkage analysis of this region in the entire family using SimWalk2 gave a location score of 4.1 (Figure 3B).

The 5' boundary marker rs2323659 is located on the p arm of the chromosome. The next informative marker, rs1589464 is separated from the boundary marker by approximately 10Mb including the centromere. At the other end of the linked region, the recombination event in individual IV:11 occurred between rs952540 and rs967293. These markers are separated by approximately 370 kb, and this region contains minimal annotated genes. Thus further fine mapping of the linked region is unwarranted.

Exome sequencing

All detected variants not present in dbSNP131 are described in the Supplement (eTable 2). Only 3 variants showed segregation in the 5 whole exome-sequenced individuals: rs118038927 at ubiquitin-specific peptidase 22 (*USP22*; GeneBank NM_015276.1), rs139539715 in the non-coding RNA *FOXO3B* (GeneBank NM_001455.3) and a novel variant at *Transmembrane protein 98* (*TMEM98*). Of these, rs118038927 is silent and has no predicted effect on protein function and rs139539715 is a common variant (minor allele frequency of 35%). Thus, the novel variant in *TMEM98* is the only variant meeting the criteria for a disease-causing variant. It is a substitution at position c.577G>C (NM_015544) leading to change of the amino acid alanine to proline at codon 193 (p.Ala193Pro) (Figure 4). This variant was shown by direct sequencing in the remainder of the family to segregate completely with disease in this family. The variant is not present in dbSNP v.137, and was not reported in the Exome Variant Server database (as of March 31, 2014). The mutation introduced a restriction site for Bsu36I resulting in bands of 180 and 420 base pairs (bp) and the undigested wildtype product was 600bp. The mutation was not present in 285 unaffected unrelated Australian white controls assessed with this restriction enzyme.

PolyPhen-2, SIFT and MutationTaster were used to predict the likely pathogenicity of this novel missense variant. MutationTaster predicted it to be a disease-causing variant; SIFT predicted the mutation to be damaging with a score of 0.05; and PolyPhen-2 predicted this mutation to be possibly damaging, with a score of approximately 60% (sensitivity 81% and specificity 83%) under the HumVar algorithm. [19]

Sequence alignment between multiple species showed a high level of conservation of the TMEM98 protein in the region of the mutation between mammals, amphibians and fish.

Conservation was less apparent with the one bird species accessed (zebra finch). The wild-type residue was found to be conserved among all vertebrates accessed as shown in the Supplement (eFigure 1).

Gene screening in additional families with nanophthalmos

Additional white families with non-syndromic nanophthalmos were recruited. Of the 22 available family members from 7 families, 13 were affected.

Two families showed autosomal dominant inheritance and, the remainder, appear to be recessive. All patients presented with short axial length with a mean of 18.8mm (1.2) and severe hyperopia with a mean of +8.4 (4) D. No novel variants in *TMEM98* were detected in the probands. All polymorphic variants identified in *TMEM98* in the probands are presented in the Supplemental (eTable 3).

Expression analysis

There are two reported transcript isoforms of *TMEM98* with different 5' UTRs (untraslated region); however both isoforms encode the same protein. The expression of both transcripts of *TMEM98* in ocular tissues was assessed by RT-PCR (eFigure 2). Both transcripts were expressed in all eye tissues assessed (ie, corneal endothelium, iris, ciliary body, sclera, optic nerve, optic nerve head, and retina) and resulted in products of the expected size (576bp for isoform 1 and 562bp for isoform 2). Direct sequencing revealed complete alignment with the reference sequence confirming the specificity of the products. Ocular expression was further confirmed using The Ocular Tissue Database (https://genome.uiowa.edu/otdb/) which showed the expression of *TMEM98* to be high in sclera, choroid RPE, iris, and ciliary body, which are believed to be involved in the pathogenesis of nanophthalmos. [23] According to the Illumina Human BodyMap data *TMEM98* is expressed in all 16 tissues tested including

adrenal, adipose, brain, breast, colon, heart, kidney, liver, lung, lymph, ovary, prostate, skeletal muscle, testes, thyroid, and white blood cells.

Discussion

In the present study, we evaluate a large pedigree of white background with autosomal dominant nanophthalmos, identifying a coding mutation in the *TMEM98* gene on chromosome 17 that likely accounts for the phenotype. The single novel segregating missense mutation, p.Ala193Pro mutation in *TMEM98*, is predicted to be damaging. Given the lack of other segregating putatively functional variants, p.Ala193Pro is likely to be the causative mutation in family NNO-SA1. In addition, the mutation was not detected in 285 indivduals, and it is not present in large public databases, strengthening the hypothesis that *TMEM98* is the most likely cause of nanophthalmos in this family. However, the absence of pathogenic variants in additional families with nanophthalmos suggests that other genetic loci for this disorder are yet to be identified and replication of this finding in an independent family is yet to occur.

The *TMEM98* gene is expressed in all eye tissues that were assessed in the present study as well as in all the human tissues tested in the Illumina Body Map project. This ubiquitous expression suggests a fundamental role in cellular processes, however, systemic effects of the mutation in family NNO-SA1 were not noted. Tissue specific effects may develop through interaction with other ocular specific transcripts during ocular development or through tissue specific splicing and regulatory mechanisms. Both isoforms analysed were expressed in the sclera. This is significant because sclera is abnormally thick in the NNO-SA1 patients and in nanophthalmos patients in general. The gene was also expressed in tissues of the iridocorneal angle including the iris and ciliary body. This expression indicates that *TMEM98* might be

involved in causing angle closure glaucoma in patients with nanophthalmos. Very little is known about the function of *TMEM98*. The encoded protein is 226 amino acids long, is leucine rich (13.3%), and is highly acidic, with a theoretical pI of 4.81; [24] it has been detected in most healthy tissues (localized to the nucleus and cytoplasm) as well as in cancers. (http://www.proteinatlas.org/ENSG00000006042/tissue).

A similar linkage region ranging from 14.1Mb to 33.0 Mb on chromosome 17, has been reported [13] in autosomal-dominant congenital simple microphthalmia in a Chinese family. The region reported in our study is entirely encompassed within the previously reported region. The overall phenotype appears similar to that described in the linked Chinese family [25], although the white family has slightly worse refraction (mean. +11.8 D vs +8.0 D) and correspondingly slightly shorter axial length (mean, 17.6 mm vs 19.2 mm). Rates of glaucoma are similar between the 2 families. The distinction between nanophthalmia and microphthalmia is likely to be arbitrary, however, molecular genetic diagnosis may help better define such overlapping conditions. It is possible that the causative gene is different between the 2 families, but it is highly likely that both conditions are caused by a mutation in the same gene within the smaller region defined by the white family reported in the present study.

Conclusion

To our knowledge, this is the first study to report mutations in *TMEM98*, and to link this gene to a disease. Additional in-depth investigations are required to explore the involvement of *TMEM98* in normal eye development and determine its role in the pathogenesis of nanophthalmos.

Acknowledgment

We thank the families who contributed samples for this project. We are grateful to the ophthalmologists who assisted with patient and family recruitment; Prof Robert Casson, Dr Mark Walland, Dr Guy D'Mellow, Dr Richard Mills, Dr Stewart Lake, Dr Michael Coote, Professor Ravi Thomas, and Dr Anna Galanopoulos. This work was funded by a grant from Flinders University and the Ophthalmic Research Institute of Australia. KPB is funded by a National Health and Medical Research Council (NHMRC) of Australia Career Development Award and JEC is an NHMRC Practitioner Fellow. Funding agencies had no role in the design and conduct of the study, collection, management, analysis or interpretation of the data, preparation, review or approval of manuscript or the decision to submit.

Author Contributions:

Drs Awadalla and Burdon contributed equally to the study. Drs had full access to all the data in the study and take responsibility for the integrity of the data and the accuracy of the data analysis.

Study concept and design: Awadalla, Burdon, Landers, Hewitt, Craig.

Acquisition, analysis, or interpretation of data: All authors.

Drafting of the manuscript: Awadalla, Burdon, Sharma, Craig.

Critical revision of the manuscript for important intellectual content: All authors.

Statistical analysis: Awadalla, Burdon.

Obtained funding: Craig.

Administrative, technical, or material support: Souzeau, Craig.

Study supervision: Burdon, Hewitt, Sharma, Craig

Conflict of interest

The authors declare that they have no conflict of interest.

Funding/Support:

This work was funded by a grant from Flinders University and the Ophthalmic Research Institute of Australia. KPB Dr Burdon receives funding from is funded by a National Health and Medical Research Council (NHMRC) of Australia Career Development Award, and JEC Dr Craig is an NHMRC practitioner fellow. National Health and Medical Research Council, Centre for Research Excellence Grant GNT1023911

Role of the Sponsor:

The sponsors had no role in the design and conduct of the study; collection, management, analysis, and interpretation of the data; preparation, review, or approval of the manuscript; and decision to submit the manuscript for publication.

Additional Contributions:

We thank the families who contributed samples for this project. We are grateful to the ophthalmologists who assisted with patient and family recruitment: Casson: MBBS, D.Phil, FRANZCO, Walland: MBBS, FRANZCO, D'Mellow: MBBS, FRANZCO, Mills: MBBS, PhD, FRANZCO, Lake:MBBS, FRANZCO, Coote: MBBS, FRANZCO, Thomas: MD, FRANZCO, Galanopoulos: MBBS, FRANZCO. The contributors did not receive financial compensation

References

1. Said, M.B., E. Chouchene, S.B. Salem, K. Daoud, L. Largueche, W. Bouassida, et al., Posterior microphthalmia and nanophthalmia in Tunisia caused by a founder c.1059_1066insC mutation of the PRSS56 gene. *Gene*, 2013.
2. Vingolo, E.M., K. Steindl, R. Forte, L. Zompatori, A. Iannaccone, A. Sciarra, et al., Autosomal dominant simple microphthalmos. *J Med Genet*, 1994. 31(9): p. 721-5.
3. Sundin, O.H., S. Dharmaraj, I.A. Bhutto, T. Hasegawa, D.S. McLeod, C.A. Merges, et al., Developmental basis of nanophthalmos: MFRP is required for both prenatal ocular growth and postnatal emmotropization. *Ophthalmic Genet*, 2008. 29: p. 1-9.
4. Sundin, O.H., G.S. Leppert, E.D. Silva, J.M. Yang, S. Dharmaraj, I.H. Maumenee, et al., Extreme hyperopia is the result of null mutations in MFRP, which encodes a Frizzled-related protein. *Proceedings of the National Academy of Sciences of the United States of America*, 2005. 102(27): p. 9553-8.
5. Khan, A.O., Recognizing posterior microphthalmos. *Ophthalmology*, 2006. 113(4): p. 718.
6. Khairallah, M., R. Messaoud, S. Zaouali, S. Ben Yahia, A. Ladjimi, and S. Jenzri, Posterior segment changes associated with posterior microphthalmos. *Ophthalmology*, 2002. 109(3): p. 569-74.
7. Spitznas, M., E. Gerke, and J.B. Bateman, Hereditary posterior microphthalmos with papillomacular fold and high hyperopia. *Arch Ophthalmol*, 1983. 101(3): p. 413-7.
8. Nowilaty, S.R., A.O. Khan, M.A. Aldahmesh, K.F. Tabbara, A. Al-Amri, and F.S. Alkuraya, Biometric and molecular characterization of clinically diagnosed posterior microphthalmos. *Am J Ophthalmol*, 2013. 155(2): p. 361-372 e7.
9. Annual Report 2010 With Data for 2008. Italy: International Clearing House for Birth Defects Surveillance and Research; 2010.
10. Martorina, M., Familial nanophthalmos. *J Fr Ophtalmol*, 1988. 11(4): p. 357-61.
11. Othman, M.I., S.A. Sullivan, G.L. Skuta, D.A. Cockrell, H.M. Stringham, C.A. Downs, et al., Autosomal dominant nanophthalmos (NNO1) with high hyperopia and angle-closure glaucoma maps to chromosome 11. *Am J Hum Genet*, 1998. 63(5): p. 1411-8.
12. Li, H., J.X. Wang, C.Y. Wang, P. Yu, Q. Zhou, Y.G. Chen, et al., Localization of a novel gene for congenital nonsyndromic simple microphthalmia to chromosome 2q11-14. *Hum Genet*, 2008. 122(6): p. 589-93.
13. Hu, Z., C. Yu, J. Li, Y. Wang, D. Liu, X. Xiang, et al., A novel locus for congenital simple microphthalmia family mapping to 17p12-q12. *Invest Ophthalmol Vis Sci*, 2011. 52(6): p. 3425-9.
14. Abecasis, G.R., S.S. Cherny, W.O. Cookson, and L.R. Cardon, Merlin--rapid analysis of dense genetic maps using sparse gene flow trees. *Nature Genetics*, 2002. 30(1): p. 97-101.
15 Mukhopadhyay, N., L. Almasy, M. Schroeder, W.P. Mulvihill, and D.E. Weeks, Mega2: data-handling for facilitating genetic linkage and association analyses. *Bioinformatics*, 2005. 21(10): p. 2556-7.
16. Sobel, E. and K. Lange, Descent graphs in pedigree analysis: applications to haplotyping, location scores, and marker-sharing statistics. *American journal of human genetics*, 1996. 58(6): p. 1323-37.
17. Wang, K., M. Li, and H. Hakonarson, ANNOVAR: functional annotation of genetic variants from high-throughput sequencing data. *Nucleic Acids Res*, 2010. 38(16): p. e164.

18. Bell, J.R., A Simple Way to Treat PCR Products Prior to Sequencing Using ExoSAP-IT®. *Biotechniques*, 2008. 44(6): p. 834.
19. Laakso, J., T. Vaskonen, E. Mervaala, H. Vapaatalo, and R. Lapatto, Inhibition of nitric oxide synthase induces renal xanthine oxidoreductase activity in spontaneously hypertensive rats. *Life Sci*, 1999. 65(25): p. 2679-85.
20. Sinisalo, J., H. Vanhanen, P. Pajunen, H. Vapaatalo, and M.S. Nieminen, Ursodeoxycholic acid and endothelial-dependent, nitric oxide-independent vasodilatation of forearm resistance arteries in patients with coronary heart disease. *Br J Clin Pharmacol*, 1999. 47(6): p. 661-5.
21. Schwarz, J.M., C. Rodelsperger, M. Schuelke, and D. Seelow, MutationTaster evaluates disease-causing potential of sequence alterations. *Nat Methods*, 2010. 7(8): p. 575-6.
22. Larkin, M.A., G. Blackshields, N.P. Brown, R. Chenna, P.A. McGettigan, H. McWilliam, et al., Clustal W and Clustal X version 2.0. *Bioinformatics*, 2007. 23(21): p. 2947-8.
23. Wagner, A.H., V.N. Anand, W.H. Wang, J.E. Chatterton, D. Sun, A.R. Shepard, et al., Exon-level expression profiling of ocular tissues. *Exp Eye Res*, 2013. 111: p. 105-11.
24. Wilkins, M.R., E. Gasteiger, A. Bairoch, J.C. Sanchez, K.L. Williams, R.D. Appel, et al., Protein identification and analysis tools in the ExPASy server. *Methods Mol Biol*, 1999. 112: p. 531-52.
25. Yu, C., Z. Hu, J. Li, T. Liu, K. Xia, and L. Xie, Clinical and genetic features of a dominantly-inherited microphthalmia pedigree from China. *Molecular vision*, 2009. 15: p. 949-54.

Figure 1: Family NNO-SA1 displaying autosomal dominant nanophthalmos. Squares indicate males, circles, indicate females, salshes, deceased individuals, blackened symbols, affected individuals. The proband is indicated with an arrow. DNA was available from individuals marked with asterisks and was included in the linkage study. Haplotypes at the linked region of chromosome 17 are shown and the segregating haplotype is black. The markers at the boundaries of recombination events are indicated and listed in the legend, along with the location of the *TMEM98* gene found to carry a mutation.

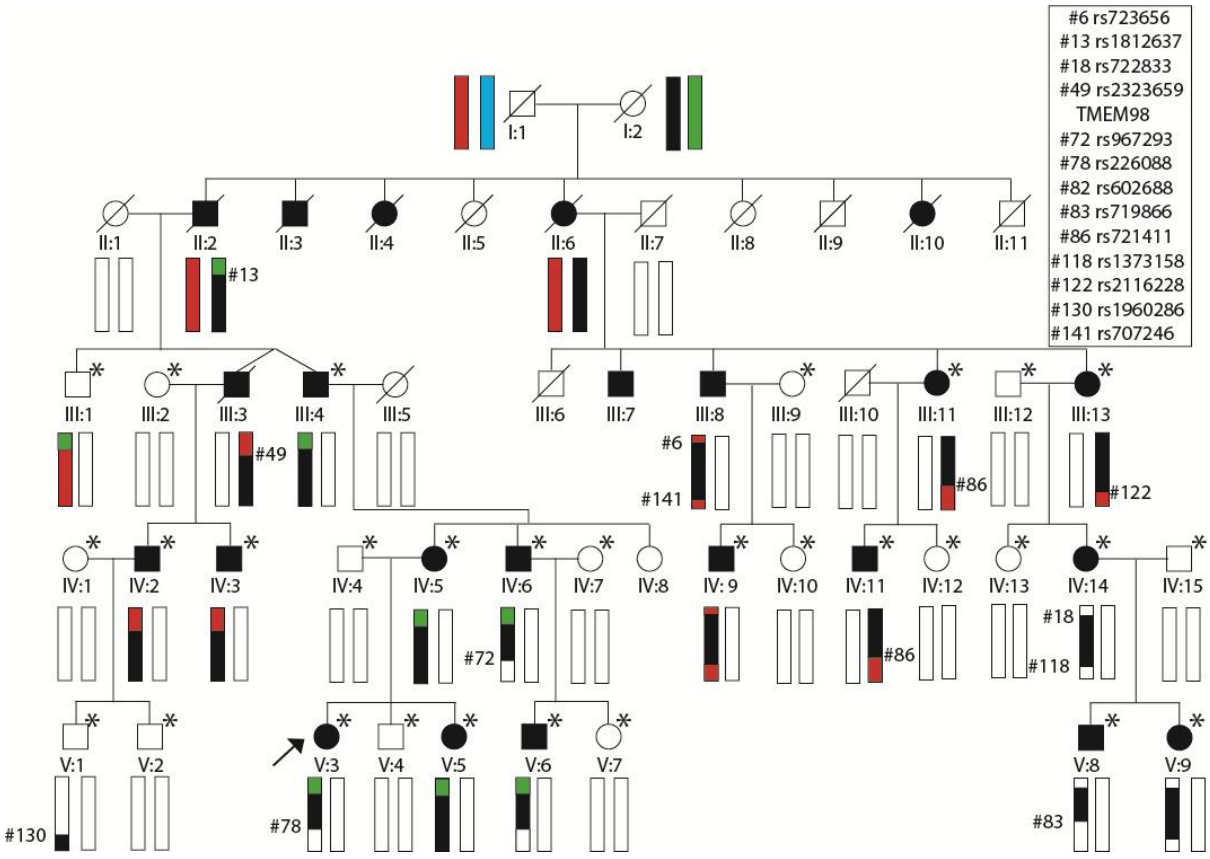

Figure 2. Clinical photos of the affected members in the Australian branch of family NNO-SA1. A, C, and E external eye appearance of patients' nanophthalmos. B, D, and F, corresponding images obtained with a rotating Scheimpflug camera system (Pentacam; Oculus). Narrow iridocorneal angles and shallow anterior chamber depth were present in all affected eyes. G, The optic disc with the presence of optic disc drusen. H, Optical coherence tomographic image of the macula showing post-operative cystoid macular edema with epiretinal membrane.

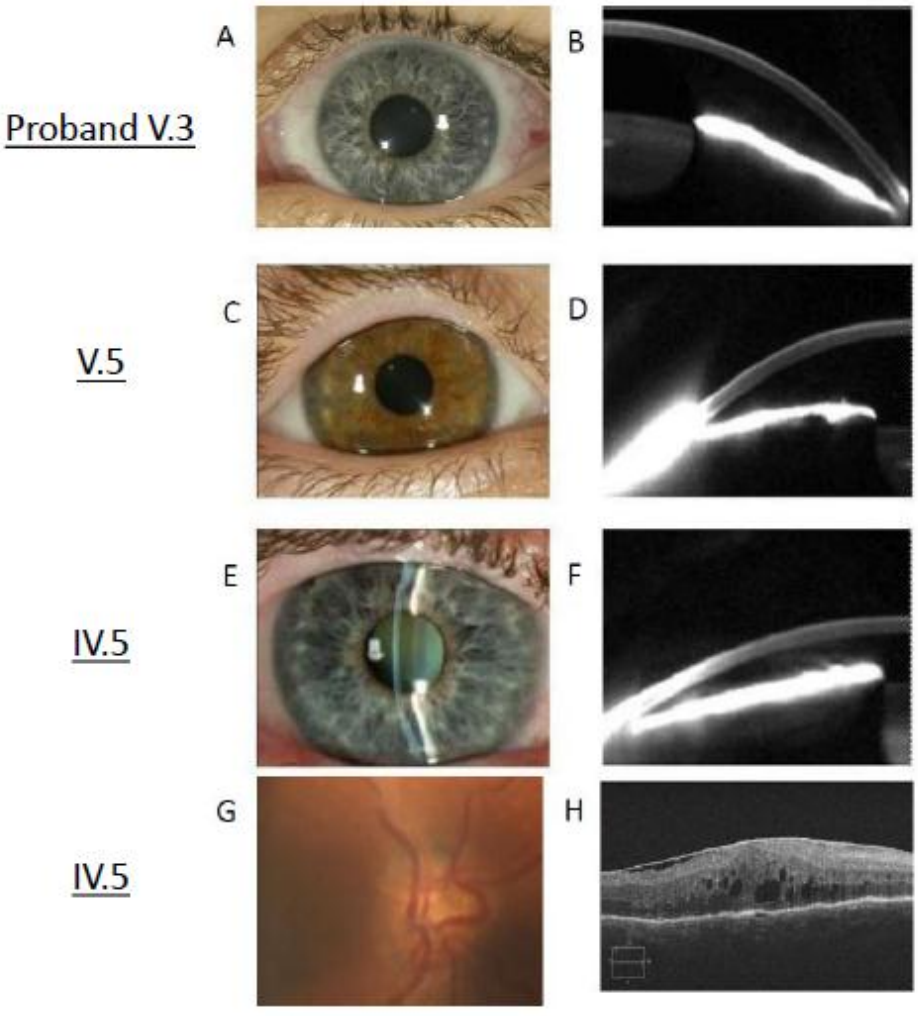

Figure 3. Linkage analysis of Family NNO-SA1

A, Linkage plot showing logarithm of odds (LOD) scores across the whole genome for the descendants of II:1 and II:2. A suggestive peak was identified on chromosome (Chr) 17. B, Linkage plot showing multi-point LOD scores (SIMWALK location scores) for the linked region of chromosome 17 (between 50 and 60 cM) in the entire family. A maximum score of 4.1 was noted at marker rs952581.

A

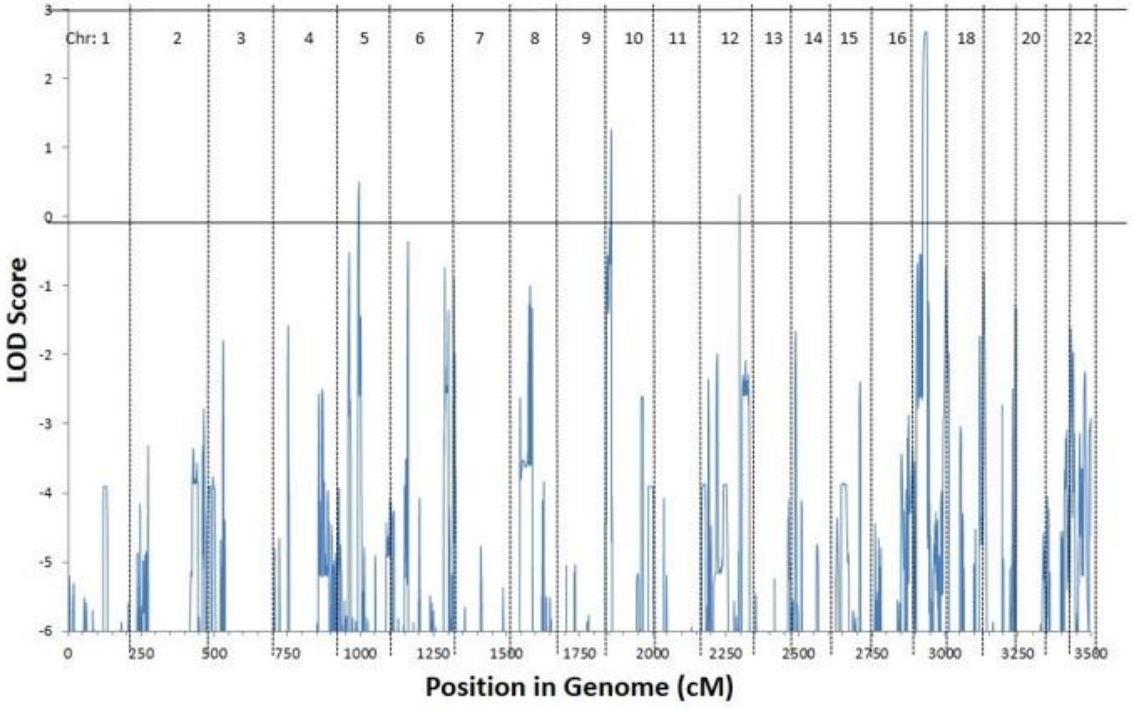
Chr: 1
2
3
4
5
6
7
8
9
10
11
12
13
14
15
16
18
20
22
LOD Score
Position in Genome (cM)

B

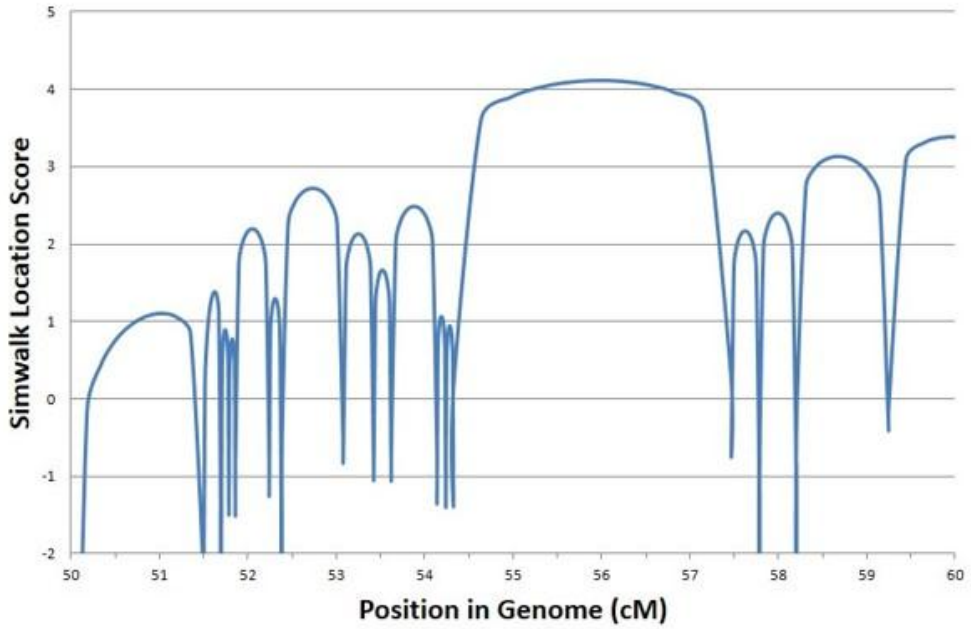
Simwalk Location Score
Position in Genome (cM)

Figure 4. Mutation located in exon 8 of *TMEM98*. A, Ideogram of *TMEM98* The black arrow indicates exon 8. B, Sequence chromatograms showing the wildtype and the novel mutation in *TMEM98* in the proband V.3 of Family 1. The red arrow indicates mutation c.577G>C (p.Ala193Pro) in the proband.

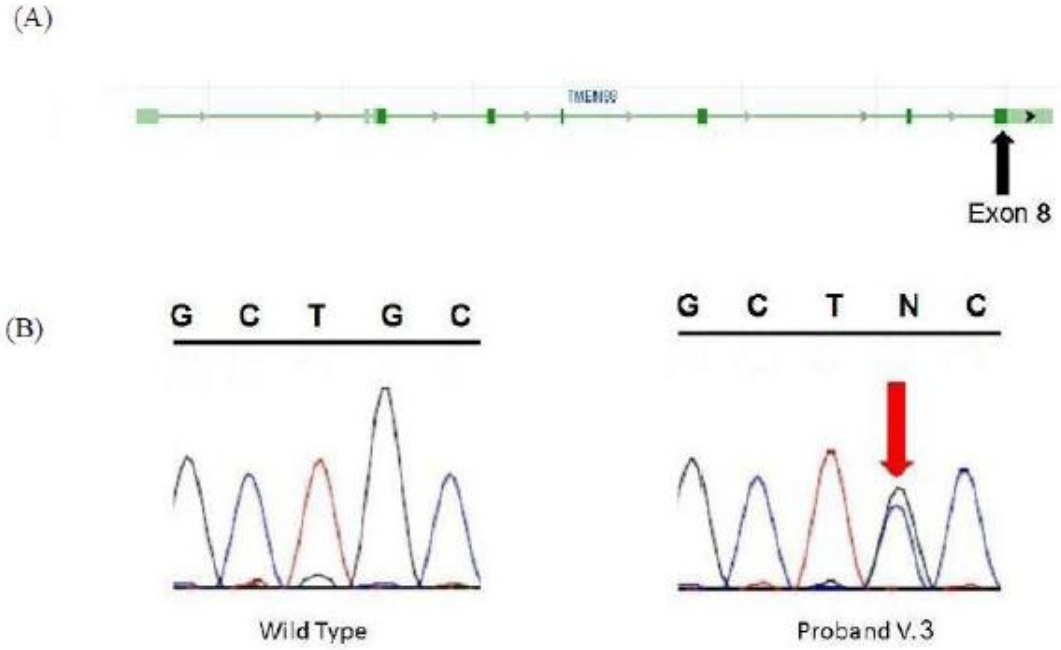

Table 1. Clinical characteristics of the affected family members.

ID	Age (years)	BCVA		Refraction (D)		Axial length (mm)		IOP (mmHg)		ACG
		RE	LE	RE	LE	RE	LE	RE	LE	
III:4	91	NA	NA	+11.5	NA	NA	NA	NA	NA	NA
III:8	78	6/24	6/30	+15.00	+15.00	18.12	17.92	13	14	No
III:11	86	HM	CF	+9.50	NA	18.02	NA	16	17	YES
III:13	84	NA	NA	+7.00	+9.50	17.43	17.31	NA	NA	YES
IV:2	64	6/6	6/9	+11.00	+11.00	17.00	NA	24	24	No
IV:3	49	6/9	6/12	+13.75	+12.87	NA	NA	18	18	NA
IV:5	61	6/48	6/12	+14.00	+15.00	17.10	17.14	33	26	YES
IV:6	63	NA	NA	+11.87	+12.37	NA	NA	18	19	No
IV:9	52	NA	NA	+9.00	+10.00	NA	NA	NA	NA	NA
IV:11	49	NA	NA	+12.50	+12.00	NA	NA	NA	NA	NA
IV:14	52	6/9	6/36	+14.25	+14.50	NA	NA	NA	NA	YES
V:3	34	6/60	6/6	+9.75	+10.50	18.46	18.34	42	41	YES
V:5	26	6/12	6/15	+15.50	+15.00	17.02	16.90	19	18	No
V:6	30	6/6	6/6	+13.25	+13.75	NA	NA	NA	NA	NA
V:8	24	6/12	NLP	+7.50	NA	18.42	NA	40	NA	YES
V:9	26	NA	NA	+8.25	+8.50	NA	NA	11	11	No

Abbreviations: ACG, angle-closure glaucoma; BCVA, best-corrected visual acuity; CF, counting fingers; D, diopters; HM, hand movements; ID, identification; IOP, highest recorded intraocular pressure; LE, left eye; NA, not available; NLP, no light perception RE, right eye.